European Conference on Optical Communication (ECOC) 2022 © Optica Publishing Group 2022

Net-bit rate of >562-Gb/s with 32-GBaud Probabilistically Constellation-Shaped 1024QAM Signal Based on Entropy and Code-Rate Optimization

Masanori Nakamura, Fukutaro Hamaoka, Takeo Sasai, Minami Takahashi, Takayuki Kobayashi, Yoshiaki Kisaka, and Yutaka Miyamoto

NTT Network Innovation Laboratories, NTT Corporation, 1-1 Hikari-no-oka, Yokosuka, Kanagawa, Japan, masanori.nakamura.cu@hco.ntt.co.jp

Abstract *We achieved a 17.57-bit/4Dsymbol information rate with >562-Gb/s net rate based on precisely entropy and code-rate optimized 32-GBaud probabilistically constellation-shaped (PCS-)1024QAM with an ultra-narrow-linewidth 1-Hz laser. A net rate of >542-Gb/s with an optimized PCS-1444QAM-based signal was also demonstrated for 30-km transmission. ©2022 The Author(s)*

Introduction

The spectral efficiency of digital coherent optical transceivers has been increased by using an advanced modulation format based on information theory alongside the ongoing progress of optoelectronic device technologies and digital signal processing.

A higher-order QAM signal with a high information rate is required to further increase the spectral efficiency. The spectral efficiency of 15.3 bit/s/Hz for 3-GBaud probabilistically constellation-shaped (PCS)-4096QAM signal using an optical phase-locked loop has been reported [1] and the spectral efficiency of 17.3-bit/s/Hz with 3-GBaud PCS-4096QAM signal has also been demonstrated by applying an ultra-narrow linewidth laser to mitigate the impact of laser phase noise [2]. The generation of high-speed and higher-order QAM signal is also challenging for signals over 1024QAM. Figure 1 shows digital coherent experiments for high information rate over 12 bit/4D-symbol. The information rates of 18 bit/4D-symbol with 15-GBaud geometrically shaped 2048QAM signal [3], 16 bit/4D-symbol with 30-GBaud PCS-4096QAM signal [4], and 22.8 bit/4D-symbol with 10-GBaud PCS-16834QAM signal [5] have been generated with a high-speed CMOS DAC.

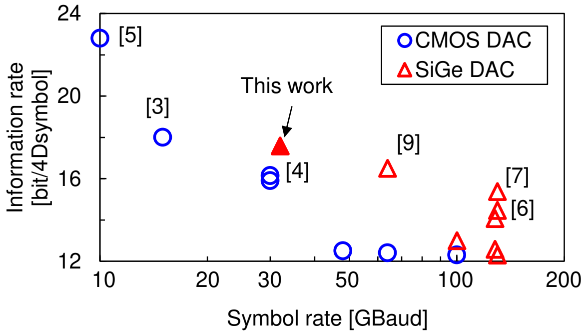

Fig. 1: Results of digital coherent experiment for high information rate over 12 bit/4D-symbol.

Recently, the information rate of 14.46 bit/4D-symbol PCS-400QAM signal [6] and 15.38 bit/4D-symbol PCS-400QAM [7] signal have been reported by using a high-speed SiGe DAC [8]. In our previous work, we demonstrated the information rate of 16.1 bit/symbol for 64-GBaud PCS-1024QAM signal generation and detection [9] by using a high-speed SiGe DAC. To further increase the information rate, we need to improve the SNR improvement and optimize the symbol probability distribution for PCS-QAM [6]. The approach for this is to use lower symbol rate PCS-QAM signals to optimize the entropy and code rate.

In this study, we optimized the PCS-QAM parameters including constellation size, entropy and ford error correction (FEC) code rate to maximize the information rate of the 32-GBaud signal generated by high-speed SiGe DAC and an ultra-narrow-linewidth 1-Hz laser. As a result, we achieved a 17.57-bit/4D-symbol information rate with a >562-Gb/s net rate based on 32-GBaud PCS-1024QAM, as shown in Fig. 1. A net rate of >542-Gb/s with a PCS-1444QAM-based signal was also demonstrated for 30-km transmission.

Information rate maximization for probabilistic amplitude shaping with entropy and code-rate optimization

In probabilistic amplitude shaping (PAS) [10], the net-bit rate C at a polarization multiplexed signal is obtained by

$$C = [H - (1 - R_c) \cdot 4m] \cdot \frac{B}{1 + P_{OH}/100}, \qquad (1)$$

where H is the entropy of constellation per 4D symbol, R_c is the FEC code rate, m is the bit number per 1D symbol, B is the symbol rate, and P_{OH} is the pilot overhead. Information rate is defined as the net-bit rate divided by the symbol rate. When we fix the symbol rate and pilot overhead, the information rate can be maximized by optimizing m, H, and R_c. H is derived from the probability distribution of the symbol with a discrete Maxwell Boltzmann (MB) distribution generated by the probabilistic amplitude shaping scheme with constant composition distribution matcher (CCDM) [10]. The shaping gain can be obtained by changing the probability distribution of the symbol in accordance with the MB distribution. However, since PCS gets signal peak-to-power average ratio (PAPR) higher, it would cause SNR degradation under the amplitude-constrained condition with the finite resolution of the DACs. Thus, we need to reveal the range of an entropy H where the shaping gain outperforms the SNR deterioration. We then determine the required code rate R_c for error-free decoding at the condition of the probability distribution. Finally, we calculate the information rate by using the H of the probability distribution and the code rate R_c. The same procedure is repeated until the information rate is maximized by changing the probability distribution.

Experimental setup

We investigated the effect of maximizing the information rate of the 32-GBaud PCS-QAM signal. Figure 2 shows the experimental setup for the evaluation. The configurations of the transmitter and receiver were the same as those for the 64-GBaud PCS-1024QAM signal [9] except for the laser diode (LD), local oscillator (LO), and part of the Tx/Rx DSP algorithms. In this experiment, we eliminated the effect of laser phase noise by using ultra-narrow linewidth 1-Hz lasers (OEwaves OE4030) as LD and LO.

At the Tx-DSP, PCS-1024QAM signals were generated by the PAS scheme with CCDM [10]. The 1444QAM, 1936QAM, and 2500QAM signals were generated by a truncated PCS-QAM scheme [11] based on the Gray mapped 4096QAM constellation. A symbol sequence with the length of 2^{17} was up-sampled using a root-raised-cosine filter with a roll-off factor of 0.01. Tx-side nonlinearity compensation (TxNLC) was carried out using a third-order Volterra filter with the same filter coefficients as [9]. On the Tx side, radio frequency (RF) signals were generated by using a SiGe-DAC-based arbitrary waveform generator (AWG) operating at 128 GSa/s. Single-ended linear driver amplifiers with a gain of 11 dB were used to drive the RF signals for the lithium-niobate-based polarization-division-multiplexed in-phase-and-quadrature modulator (PDM-IQM). The PDM-QAM signal was modulated with a carrier signal of 193.755 THz output from an ultra-narrow linewidth 1Hz laser amplified up to 25.5 dBm using an erbium-doped fibre amplifier

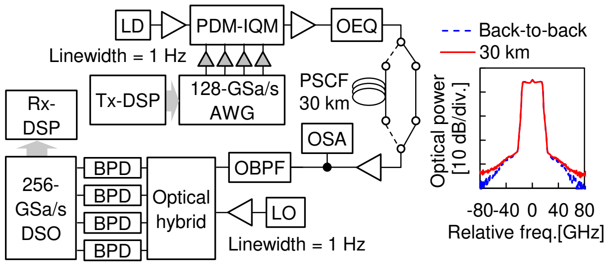

Fig. 2: Experimental setup.

(EDFA). Optical equalization (OEQ) was carried out for the modulated optical signals. The optical spectra measured by an optical spectrum analyser (OSA) at the back-to-back and after 30-km pure-silica core fibre (PSCF) transmission at a launched power of -2 dBm are shown in Fig. 2.

At the Rx side, the received signal was amplified using an EDFA and filtered by an optical bandpass filter (OBPF). The signals were detected by a coherent receiver composed of an optical hybrid and four balanced photo detectors (BPDs). A 256-GSa/s digital storage oscilloscope (DSO) digitized the received signal.

At the Rx-DSP, the sampling rate of the signal was converted into two samples per symbol. Then, compensation for the linear responses in the Tx and Rx, frequency offset compensation, and carrier phase recovery were simultaneously carried out using a frequency domain 8×2 MIMO adaptive equalizer [9] utilizing a pilot-based digital phase-locked loop with a pilot overhead of 1.78%. The log-likelihood ratios (LLRs) were calculated using a bit-metric decoder [10]. Finally, we evaluated the constellation SNR, generalized mutual information (GMI), and normalized GMI (NGMI) [12].

Experimental results and discussion

First, we measured the SNR after demodulation for each probability distribution for the 1024QAM, 1444QAM, 1936QAM, and 2500QAM, as shown in Fig. 3(a). As we can see, the SNR of each QAM with a uniform distribution signal is the highest, and it decreases with the constellation shaping. We then evaluated the GMIs for each QAM signal, as shown in Fig. 3(b), where the GMI curve of each QAM size has a peak due to the balance between the shaping gain and the SNR degradation.

Next, we determined the required code rate R_c for error-free decoding at the condition of the probability distribution of each QAM by using the offline evaluation scheme [13]. We used the DVB-S2 LDPC codes [14] with a codeword length of 64800 and code rate of 5/6. The rate-adaptive coding [15] was performed by puncturing the base on the above code rate. Figure 3(c) shows the post-LDPC bit-error rates as a function of the

LDPC overhead for each QAM at the condition of the maximum GMI as an example. We examined about 300 codewords for LDPC decoding by using the LLRs. We assumed an outer hard-decision (HD-)FEC with the code rate of 0.9922 and a BER threshold of 5×10^{-5} [16]. Error-free decoding can be achieved when the post-LDCP BER is less than the HD-FEC threshold. The required FEC code rate R_c was calculated by concatenating the code rates of the LDPC codes and outer HD-FEC codes. The required code rate and NGMI in each QAM with a different symbol probabilistic distribution are shown in Fig. 3(d). The code rate needs to be bigger than $\frac{m-1}{m}$ for the PAS scheme, as the parity bits must be assigned as sign bits of the 1D symbols [10]. For 4096QAM-based truncated PCS-QAM, the code rate is equal to or higher than 5/6. No error-free condition was found for the 2500QAM because the measured NGMIs were close to 5/6, as shown in Fig. 3(d). Figure 3(e) shows the achievable bit rate derived from the GMI and the net-bit rate calculated from the required code rate. These bit rates were calculated excluding pilot overhead. When compared with the achievable bit rate, the bit rate was the highest at the PCS-1936QAM. In contrast, when compared with net-bit rate, the PCS-1024QAM achieved the highest rate. This is because the impact of the implementation penalty of the practical FEC decreases at PCS-1024QAM, whose $m = 5$ compared to PCS-4096QAM, whose $m = 6$ [17]. The maximum net-bit rate was 562.5 Gb/s at the condition of PCS-1024QAM with the entropy of 19.743 bit/4D-symbol and the code rate of 0.9075. The information rate was 17.57 bit/4D-symbol.

Finally, we evaluated the net-bit rate for truncated PCS-1444QAM after 30-km transmission in the same manner. The maximum bit rate of the PCS-1444QAM was >542 Gb/s, as shown in Fig. 3(f). This result shows that the optimization scheme can be applied to the PCS-QAM signal even after fibre transmission in the linear regime.

Conclusions

We achieved a 17.57-bit/4D-symbol information rate with a >562-Gb/s net rate based on 32-GBaud PCS-1024QAM thanks to the entropy of the symbol probabilistic distribution and code-rate optimization by using adaptive coding scheme and an ultra-narrow-linewidth 1-Hz laser. An information rate of 16.93-bit/4D-symbol with a >542-Gb/s net rate signal with a PCS-1444QAM was also demonstrated for 30-km PSCF transmission.

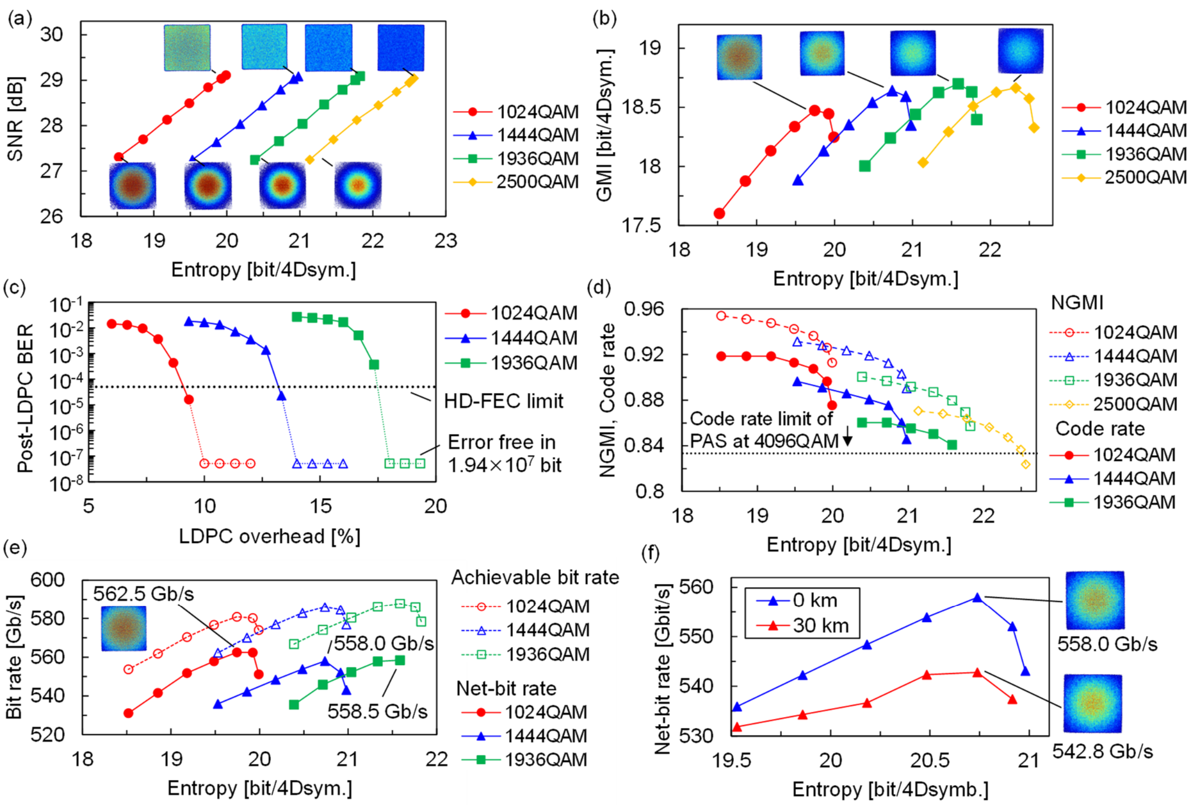

Fig. 3: Experimental results of (a) SNR vs. entropy, (b) GMI as a function of entropy, (c) post-LDPC BER vs. LDPC overhead, (d) NGMI and code rate as a function of entropy, (e) bit rate as a function of entropy and (f) net-bit rate of truncated PCS-1444QAM as a function entropy at 0 km and transmission over 30-km PSCF.

References

[1] S. Okamoto, M. Terayama, M. Yoshida, K. Kasai, T. Hirooka, and M. Nakazawa, "Experimental and numerical comparison of probabilistically shaped 4096 QAM and a uniformly shaped 1024 QAM in all-Raman amplified 160 km transmission," *Optical Express*, vol. 26, no. 3, pp. 3535-3543, 2018, DOI: 10.1364/OE.26.003535

[2] S. Olsson, J. Cho, S. Chandrasekhar, X. Chen, E. C. Burrows, and P. J. Winzer, "Record-high 17.3-bit/s/Hz spectral efficiency transmission over 50 km using PS-PDM 4096-QAM," in *Proceedings Optical Fiber Communication Conference (OFC)*, San Diego, CA, USA, 2018, Th4C.5. DOI: 10.1364/OFC.2018.Th4C.5

[3] Y. Wakayama, T. Gerard, E. Sillekens, L. Galdino, D. Lavery, R. I. Killey, and P. Bayvel, "2048-QAM transmission at 15 GBd over 100 km using geometric constellation shaping," *Optics Express,* vol. 29, no. 12, pp. 18743-18759, 2021, DOI: 10.1364/OE.423361

[4] X. Chen, S. Chandrasekhar, J. Cho, and P. Winzer, "Transmission of 30-GBd polarization-multiplexed probabilistically shaped 4096-QAM over 50.9-km SSMF," *Optics Express,* vol. 27, no. 21, pp. 29916-29923, 2019, DOI: 10.1364/OE.27.029916

[5] X. Chen, J. Cho, A. Adamiecki and P. Winzer, "16384-QAM transmission at 10 GBd over 25-km SSMF using polarization-multiplexed probabilistic constellation shaping," in *Proceedings The European Conference on Optical Communication (ECOC)*, Dublin, Ireland, 2019, pp. 1-4, DOI: 10.1049/cp.2019.1030

[6] F. Pittalà, R. Braun, G. Böcherer, P. Schulte, M. Schaedler, S Bettelli, S. Calabrò, M. Kuschnerov, A. Gladisch, F. Westphal, C. Xie, R. Chen, Q. Wang, and B. Zheng,"1.71 Tb/s Single-Channel and 56.51 Tb/s DWDM Transmission Over 96.5 km Field-Deployed SSMF," *IEEE Photonics Technology Letters*, vol. 34, no. 3, pp. 157-160, 1 Feb.1, 2022, DOI: 10.1109/LPT.2022.3142538

[7] M. Xu, Y. Zhu, F. Pittalà, J. Tang, M. He, W. C. Ng, J. Wang, Z. Ruan, X. Tang, M. Kuschnerov, L. Liu, S. Yu, B. Zheng, and X. Cai, "Dual-polarization thin-film lithium niobate in-phase quadrature modulators for terabit-per-second transmission," *Optica*, vol. 9, pp. 61-62, 2022, DOI: 10.1364/OPTICA.449691

[8] F. Buchali, V. Aref, R. Dischler, M. Chagnon, K. Schuh, H. Hettrich, A. Bielik, L. Altenhain, M. Guntermann, R. Schmid, and M. Möller, "128 GSa/s SiGe DAC Implementation Enabling 1.52 Tb/s Single Carrier Transmission," *Journal of Lightwave Technology*, vol. 39, no. 3, pp. 763-770, 2021, DOI: 10.1109/JLT.2020.3034535

[9] M. Nakamura, T. Kobayashi, F. Hamaoka and Y. Miyamoto, "High Information Rate of 128-GBaud 1.8-Tb/s and 64-GBaud 1.03-Tb/s Signal Generation and Detection Using Frequency-Domain 8×2 MIMO Equalization," in *Proceedings Optical Fiber Communication Conference (OFC)*, San Diego, CA, USA, 2022, M3H.1, DOI: 10.1364/OFC.2022.M3H.1

[10] G. Böcherer, F. Steiner and P. Schulte, "Bandwidth Efficient and Rate-Matched Low-Density Parity-Check Coded Modulation," *IEEE Transactions on Communications*, vol. 63, no. 12, pp. 4651-4665, 2015, DOI: 10.1109/TCOMM.2015.2494016

[11] I. Fernandez de Jauregui Ruiz, A. Ghazisaeidi, O. A. Sab, P. Plantady, A. Calsat, S. Dubost, L. Schmalen, V. Letellier, and J. Renaudier,, "25.4-Tb/s Transmission Over Transpacific Distances Using Truncated Probabilistically Shaped PDM-64QAM," *Journal of Lightwave Technology*, vol. 36, no. 6, pp. 1354-1361, 2018, DOI: 10.1109/JLT.2018.2791615

[12] J. Cho, L. Schmalen and P. J. Winzer, "Normalized Generalized Mutual Information as a Forward Error Correction Threshold for Probabilistically Shaped QAM," in *Proceedings The European Conference on Optical Communication (ECOC)*, 2017, pp. 1-3, DOI: 10.1109/ECOC.2017.8345872

[13] T. Yoshida, M. Karlsson, and E. Agrell, "Efficient Offline Evaluation of FEC Codes Based on Captured Data with Probabilistic Shaping," in *Proceedings Optical Fiber Communication Conference (OFC)*, San Diego, CA, USA, 2018, M4E.5.DOI: 10.1364/OFC.2018.M4E.5

[14] ETSI, "Digital Video Broadcasting (DVB); Second generation framing structure, channel coding and modulation systems for Broadcasting, Interactive Services, News Gathering and other broadband satellite applications," EN 302 307-1, v.1.4.1, 2014.

[15] A. Ghazisaeidi, L. Schmalen, I. Fernandez de Jauregui Ruiz, P. Tran, C. Simonneau, P. Brindel, and G. Charlet, "Transoceanic Transmission Systems Using Adaptive Multirate FECs," *Journal of Lightwave Technology*, vol. 33, no. 7, pp. 1479-1487, 2015, DOI: 10.1109/JLT.2015.2399174

[16] D. S. Millar, R. Maher, D. Lavery, T. Koike-Akino, M. Pajovic, A. Alvarado, M. Paskov, K. Kojima, K. Parsons, B. C. Thomsen, S. J. Savory, and P. Bayvel, "Design of a 1 Tb/s Superchannel Coherent Receiver," *Journal of Lightwave Technology*, vol. 34, no. 6, pp. 1453-1463, 2016, DOI: 10.1109/JLT.2016.2519260

[17] J. Cho, S. L. I. Olsson, S. Chandrasekhar, and P. Winzer, "Information rate of probabilistically shaped QAM with non-ideal forward error correction," in *Proceedings The European Conference on Optical Communication (ECOC)*, Rome, Italy, 2018, pp. 1–3, DOI: 10.1109/ECOC.2018.8535577